2013

Protein-Nanoparticle Interactions: the Effects of Surface Compositional and Structural Heterogeneity are Scale Dependent

Rixiang Huang
Randy P. Carney
Francesco Stellacci
Boris Lau, *University of Massachusetts - Amherst*

Nanoscale

RSC Publishing

PAPER

View Article Online
View Journal | View Issue

Cite this: *Nanoscale*, 2013, **5**, 6928

Protein–nanoparticle interactions: the effects of surface compositional and structural heterogeneity are scale dependent†

Rixiang Huang,[a] Randy P. Carney,[b] Francesco Stellacci[b] and Boris L. T. Lau*[ac]

Nanoparticles (NPs) in the biological environment are exposed to a large variety and concentration of proteins. Proteins are known to adsorb in a 'corona' like structure on the surface of NPs. In this study, we focus on the effects of surface compositional and structural heterogeneity on protein adsorption by examining the interaction of self-assembled monolayer coated gold NPs (AuNPs) with two types of proteins: ubiquitin and fibrinogen. This work was designed to systematically investigate the role of surface heterogeneity in nanoparticle–protein interaction. We have chosen the particles as well as the proteins to provide different types (in distribution and length-scale) of heterogeneity. The goal was to unveil the role of heterogeneity and of its length-scale in the particle–protein interaction. Dynamic light scattering and circular dichroism spectroscopy were used to reveal different interactions at pH above and below the isoelectric points of the proteins, which is related to the charge heterogeneity on the protein surface. At pH 7.4, there was only a monolayer of proteins adsorbed onto the NPs and the secondary structure of proteins remained intact. At pH 4.0, large aggregates of nanoparticle–protein complexes were formed and the secondary structures of the proteins were significantly disrupted. In terms of interaction thermodynamics, results from isothermal titration calorimetry showed that ubiquitin adsorbed differently onto (1) AuNPs with charged and nonpolar terminals organized into nano-scale structure (66-34 OT), (2) AuNPs with randomly distributed terminals (66-34 brOT), and (3) AuNPs with homogeneously charged terminals (MUS). This difference in adsorption behavior was not observed when AuNPs interacted with fibrinogen. The results suggested that the interaction between the proteins and AuNPs was influenced by the surface heterogeneity on the AuNPs, and this influence depends on the scale of surface heterogeneity and the size of the proteins.

Received 28th April 2013
Accepted 22nd May 2013

DOI: 10.1039/c3nr02117c

www.rsc.org/nanoscale

1 Introduction

The interaction between nanoparticles (NPs) and proteins is of great relevance in nanotoxicology and biomedical applications of nanomaterials. Understanding the physicochemical interaction (*e.g.*, interaction forces, binding sites and affinity) and the subsequent effects (*e.g.*, conformation and activity of the interacting proteins, stability and functionality of the NPs) is crucial for understanding the mechanism of toxicity and better design and application of nanomaterials.[1] The interaction and its subsequent effects were found to be governed by the properties of both nanomaterials and proteins, including size, shape and surface properties.[2–5]

Surface heterogeneity, the coexistence of different chemistry and structures, is ubiquitous in both natural and engineered systems.[6,7] Proteins themselves, for example, possess exposed patches of polar/nonpolar and negatively/positively charged chemical groups at the molecular scale or the nanoscale. In general, it has been found that surfaces with heterogeneous composition exhibit properties that do not change linearly with molar composition as expected by classical arguments (*e.g.*, electrokinetics,[8] interfacial forces[9] and surface tension[10]). However, a quantitative relationship between surface heterogeneity and measurable properties has not been established, and the correlation between surface heterogeneity and interfacial processes is not self-evident.

It has been recognized that surface heterogeneity is scale-dependent. For example, colloidal adhesion was found to have heterogeneity-dominated or mean-field behavior depending on the scale of surface heterogeneity.[11] The influence of surface heterogeneity on protein adsorption has been studied at the microscale.[12,13] Although the adsorption extent, adsorption

[a]*Department of Geology, Baylor University, One Bear Place #97354, Waco, Texas, 76798, USA*

[b]*Institute of Materials, Ecole Polytechnique Fédérale de Lausanne, Lausanne 1015, Switzerland*

[c]*Department of Civil and Environmental Engineering, University of Massachusetts Amherst, 224 Marston Hall, 130 Natural Resources Road, Amherst, MA 01003-9293, USA. E-mail: borislau@engin.umass.edu; Fax: +1 413-545-2840; Tel: +1 413-545-2508*

† Electronic supplementary information (ESI) available. See DOI: 10.1039/c3nr02117c

kinetics, and surface distribution of proteins are different between homogeneous and heterogeneous surfaces, the mechanisms of protein adsorption are similar, because the scale of surface heterogeneity is much larger than the size of proteins. Little is known about the effects on protein adsorption when surface heterogeneity approaches the nanoscale, comparable to the size of a single protein.

In this study, we investigated the effects of surface compositional and structural heterogeneity on protein–NP interaction using self-assembled monolayer coated AuNPs and two proteins of different sizes and shapes. The AuNPs are nearly identical in size distribution, shape, surface charge and ligand density, with quantitative differences only in the composition and arrangement of ligands on the surface.[14–16] For particles with such nanoscale surface features, interesting properties regarding wettability,[17] interfacial energy[18] and cell penetration[16] were found to be dependent on the surface composition and structure. Thus, it is important to study how these properties correlate with the adsorption behavior of proteins (ubiquitin and fibrinogen). These proteins were selected for this study because of their abundance in animal plasma and differences in size, shape, and properties.

Complementary to previous studies that used particles with different sizes and shapes but usually homogeneous surface chemistry, this study unveils the unique importance of the size of surface functionality (both on the NPs and on the proteins) in NP–protein interactions. The results of this work develop the emerging concept of "scale dependency" systematically by demonstrating that the effects of surface heterogeneity are dependent on the relative scale between protein and the NP surface features. The novel findings presented here are crucial in (1) predicting the subsequent biological activity of NP–protein complexes and (2) improving the design of novel nanomaterials for applications in various biological and environmental systems (*e.g.*, drug delivery, protein purification, and treatment of water and wastewater).

Adsorption was performed in defined aqueous solution at pH above and below the isoelectric point (IEP) of ubiquitin and fibrinogen to study the effects of surface charge, structure and exposed functional groups from proteins. The different sizes and shapes of the selected proteins and their different properties at the two pHs create different types of heterogeneity.

The surface charge of the AuNPs and the proteins was characterized by electrophoretic mobility measurements. The adsorption process was manifested through size change of the AuNPs and was monitored by dynamic light scattering (DLS). Isothermal titration calorimetry (ITC) was used to explore the thermodynamics behind the interaction. The conformational change of the proteins was monitored by circular dichroism (CD) spectroscopy. Results from individual technique were integrated to understand the mechanism of interaction.

2 Experimental section

2.1 Preparation of AuNPs and protein suspensions

The three types of ligand-coated AuNPs used in this study have been thoroughly characterized with respect to their size, surface chemical composition and structure.[15,16] AuNPs are coated with (1) all negatively charged, sulfonated alkanethiols (11-mercapto-1-undecanesulfonate, MUS), (2) a 2 : 1 molar mixture of MUS and 1-octanethiol (OT) (now referred to as 66-34 OT), and (3) a 2 : 1 molar mixture of MUS and a branched, apolar version of OT (3,7-dimethyl octane 1-thiol, brOT) (66-34 brOT). Previously we have shown that the 66-34 OT AuNPs exhibit unique properties due to the ordering of molecules in their ligand shell. To prepare the AuNP stock solutions, around 6 mg of AuNP powder was added into 20 mL of ultrapure water (Millipore Simplicity, >18 MΩ cm), the solutions were sonicated in an ultrasonic bath (VWR, B2500A-MT) for 30 min. After ultrasonication, the AuNP suspensions were centrifuged at 9000*g* (Avanti A-J., Beckman-Coulter, Brea, CA) for 30 min in order to remove nondispersive aggregates from the suspensions. The mass concentration of AuNPs was quantified by a Perkin Elmer ELAN 9000 inductively coupled plasma mass spectrometer (ICP-MS) (Waltham, MA), from which the molar concentration was derived.

Ubiquitin from bovine erythrocytes (lyophilized powder) and fibrinogen from human plasma (lyophilized powder) were purchased from Sigma and used without further purification. The stock solution of the proteins was prepared in 10 mM sodium phosphate buffer solution (PBS) of pH 7.4 and stored at 4 °C, and the stock solution was used within one week. Buffers at pH 4.0 and 7.4 were prepared using 10 mM sodium acetate–acetic acid and PBS, respectively.

2.2 Surface charge measurements

The electrophoretic mobility (EPM) of the AuNPs and proteins at various pHs was measured using a Malvern Zetasizer (Nano ZS, Malvern Instruments, UK), and converted to ζ-potentials using the Smoluchowski equation. Protein and AuNP solutions for EPM measurements were prepared by diluting the stock solution into their respective buffer solutions. The NP concentrations for EPM measurements were around 0.1–0.2 times of the concentrations of the corresponding AuNP stock suspensions. The concentration of ubiquitin and fibrinogen was around 1 μmol L^{-1}. Around 600 μL solution was pipetted into the DTS 1060C disposable capillary cell. Six measurements were conducted for duplicate samples under each condition.

2.3 Dynamic light scattering

The hydrodynamic diameter change of the AuNPs in the absence and presence of proteins was measured using the Zetasizer Nano ZS with a fixed detector angle of 173°. Specifically, at pH 7.4, protein solution was sequentially added into the AuNP suspension (around 0.05 μmol L^{-1}) to reach certain final protein–AuNP molar ratios (ubiquitin: 0 to 100; fibrinogen: 0 to 10). The mixture was incubated for 30 min before DLS measurement and 15 measurements were taken. The maximum size change was chosen for comparison. At pH 4.0, a protein to AuNP molar ratio of 10 : 1 was chosen. DLS measurements started immediately after the addition of proteins and 15 measurements were taken. The results were the average of at least two separate experiments.

2.4 Circular dichroism spectroscopy

CD measurements were undertaken by a Jasco J-810 spectropolarimeter (Easton, MD) with a 2 mm path length rectangular quartz cell at room temperature (22 °C). The CD spectra were recorded from 190 to 260 nm and each spectrum was an average of 5 scans.

The test solutions for CD were prepared by mixing the proteins and AuNPs in their respective buffer and then incubated at 4 °C for at least 30 min before the spectra were collected. The concentration of ubiquitin and fibrinogen was fixed at 1 μmol L^{-1} and 0.5 μmol L^{-1}, respectively, and the AuNP concentration ranged from 0 to 0.05 μmol L^{-1}.

2.5 Isothermal titration calorimetry

ITC measurements were performed on a MicroCal ITC200 system (GE Healthcare). Both ubiquitin and fibrinogen were dialyzed overnight against 10 mmol L^{-1} sodium phosphate buffer (renewed two times) at pH 7.4, and the AuNPs were dissolved in the last dialysate (sonicated, then centrifuged at 9000 rpm for 15 min). The titration experiment involved 40 injections (1 μl per injection) of proteins (ubiquitin concentration = 1 mmol L^{-1} and fibrinogen concentration = 80 μmol L^{-1}) at 150 s intervals into the sample cell (volume = 200 μL) containing the AuNP solution (MUS con. = 7.03 μmol L^{-1}, 66-34 brOT con. = 8.43 μmol L^{-1} and 66-34 OT con. = 7.73 μmol L^{-1}). The reference cell was filled with 10 mmol L^{-1} sodium phosphate buffer. During the experiment, the sample cell was stirred continuously at 1000 rpm. At least two separate experiments were conducted for each protein–AuNP pair.

The heat profile of protein dilution in the buffer alone was subtracted from the titration data (both normalized to 0) for each experiment. The data were analyzed to determine the binding stoichiometry (n), association constant (K_s), and other thermodynamic parameters of the reaction using the coupled Origin software. The reported thermodynamic parameters were an average of duplicate experiments.

3 Results and discussion

3.1 Characterization of the AuNPs and proteins

Detailed information regarding the synthesis and characterization can be found in our previous studies.[15,16] These three types of AuNPs were confirmed to be similar in size and shape to the ones previously synthesized.[15,16] The core diameter of the three AuNPs was 4.4 ± 0.4 nm based on the size distribution determined by TEM (Fig. S1†). The ligand shell has a thickness of 1.5 nm, making the diameter of the whole particle around 7.4 nm. The ligand shell composition was based on ^{1}H NMR analysis of the ligands after decomposition of the gold core by KCN,[19] and the ligand distribution was based on scanning tunneling microscopy (STM) performed in previous studies.[15,16] These characterizations showed that MUS particles were homogeneously coated with MUS only, 66-34 brOT were coated with randomly distributed MUS and brOT, while MUS and OT ligands were separated into stripe-like domains (~1 nm) on the surface of the 66-34 OT particles. The hydrodynamic diameter (d_h) of the AuNPs and proteins was measured by dynamic light scattering (DLS) and the results are shown in Fig. 1A. Ubiquitin, a compact protein that consists of only 76 amino acids (1.57 nm in diameter),[20,21] was too small to be reliably quantified by DLS. Fibrinogen is a high molecular weight, elongated protein (47.5 nm long), with three polypeptide domains that are around 5–6 nm in diameter.[22] Its d_h was 24.7 ± 0.4 nm. The d_h of fibrinogen was consistent with previous studies.[20,23] All proteins and AuNPs were stable in the buffer for more than 24 hours.

The electrophoretic mobility (EPM) of each of the particles and proteins was measured and converted to ζ-potential values (Fig. 1B). For the AuNPs, the terminal sulfonate groups determine the surface charge of their protecting SAMs, and the particles remain negatively charged at the two pHs. Since the IEPs of ubiquitin and fibrinogen are around 6.8 and 5.8,[23,24] respectively, the overall surface charge of ubiquitin and fibrinogen would be positive at pH 4.0 and negative at pH 7.4.

3.2 Stability of AuNP–protein complexes

DLS has been frequently used to characterize protein–nanoparticle interaction and to reveal their interaction mechanism.[25,26] The size change of AuNPs due to the addition of proteins is presented in Fig. 2. It was found that the system behaved differently at the two pHs. At pH 4.0, a size change of more than 100 nm was observed in all types of AuNPs in the presence of both types of proteins (Fig. 2A). Considering the relatively small size of the AuNPs and proteins, it is evident that large aggregates were formed at pH 4.0. It is likely that they were aggregates of AuNP–protein complexes connected by the denatured proteins initially coated on the particle surface (disruption of the secondary structure of proteins due to adsorption at pH 4.0 as shown in Section 3.3). It is noteworthy that the different size changes between different types of AuNPs may not simply be the result of AuNP surface difference, because the subsequent protein–protein interactions may have little relevance with the AuNPs. Thus, the result of these size changes should not be over-interpreted. At pH 7.4, the size changes following the addition of ubiquitin and fibrinogen were around 2 nm and 20 nm, respectively, which are comparable to the size of the proteins (Fig. 2B). These size changes suggested that the AuNPs were probably coated with a monolayer of proteins at pH 7.4. These monolayer protein-coated AuNPs were found to be stable by DLS even after 24 hours (±0.5 nm).

The different behaviors at pH above and below proteins' IEP reflect the different interaction modes between the proteins and AuNPs under different conditions. Several factors should be considered in order to identify the interaction modes. First, the overall surface charge of the proteins changed from negative to positive as pH changed from 7.4 to 4.0; second, proteins are big molecules with complex structure and heterogeneous surface, they consist of a long chain of amino acids with different side chains organized into three dimensions of structures and their surface consists of a mixture or patches of polar/nonpolar functional groups; third, the structure of protein may change as a function of pH.[27] Therefore, the AuNP–protein interface is rather dynamic, with the interaction mode depending on the surface

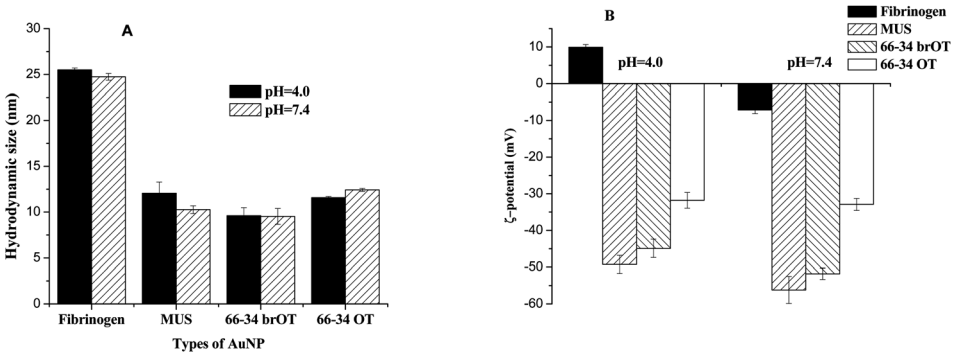

Fig. 1 (A) Hydrodynamic diameter of unbound fibrinogen and AuNPs at pH 4.0 and pH 7.4. (B) ζ-Potentials of proteins at pH 4.0 and pH 7.4.

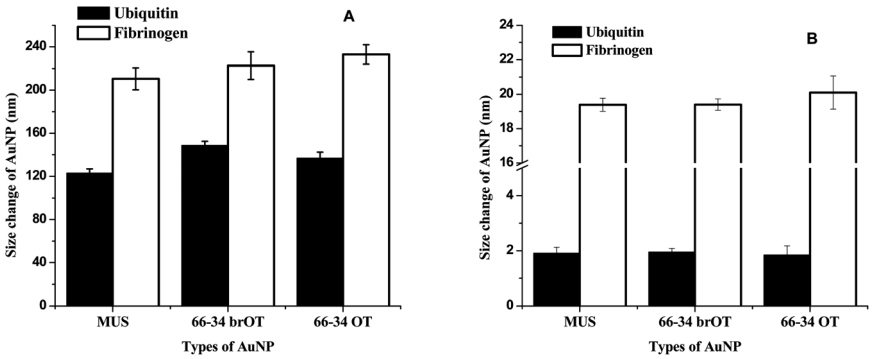

Fig. 2 The change of hydrodynamic diameter of AuNPs following the addition of proteins at pH 4.0 (A) and pH 7.4 (B), error bars represent the variations between duplicate experiments.

composition and structure of the proteins and the AuNPs, which is modulated by factors like pH and ionic strength.

All these considerations motivated the following application of spectroscopic and thermodynamic techniques to further understand protein–AuNP interactions.

3.3 Conformational change of proteins

CD spectroscopy is a powerful analytical tool to monitor the conformational change of proteins as a result of the changes in solution chemistry (*e.g.*, pH, temperature or ionic strength) or interactions with molecules or adsorption onto the particle surface. It has been frequently used to measure the structural changes induced in proteins due to interaction with nanomaterials.[2,28,29]

In this study, the α-helix structure of both proteins, which is manifested by the negative peaks at around 208 nm and 222 nm in CD spectra, was monitored. At pH 7.4, there was no significant change in the ellipticity values of the proteins in the presence of all three types of AuNPs, which indicated that the proteins maintained their conformation after adsorption onto the surface of AuNPs (Fig. 3 and 4 (right)). Since the protein conformation remained intact, they were stable against further interactions with each other. At pH 4.0, in the presence of MUS and 66-34 brOT, the ellipticity significantly decreased and the peaks at 208 nm and 222 nm disappeared, which is a sign of disruption of the secondary structure (Fig. 3 and 4 (left)). While at pH 4.0, the structural change for all types of proteins in the presence of 66-34 OT was less significant than that of MUS and 66-34 brOT.

In this study, AuNPs were coated by thiols with long carbon chains and the surface properties are only determined by the ligand shell. The negative charge of these SAM-coated AuNPs at the tested pHs was determined by the terminal $-SO_3^-$ groups. The interaction between proteins with these AuNPs was most likely directed by the positively charged regions of the proteins toward the negatively charged AuNP surface. As pH decreased from 7.4 and 4.0, more residues on the protein surface were protonated, thus there were more positively charged regions available for interaction. This may have resulted in a tighter interaction between the proteins and AuNPs, and the protein structure was more vulnerable to disruption.

With information on conformational change, it can be anticipated that formation of large aggregates under opposite charge conditions was due to the fact that AuNPs disrupted the structure of the first adsorbed layer of proteins. The disrupted proteins could interact with other unbound proteins or protein-coated AuNPs, thus initiate aggregation.

3.4 Isothermal titration calorimetry and binding thermodynamics of NP–protein interactions

ITC directly measures the binding affinity constant, enthalpy changes, and binding stoichiometry between NPs and proteins

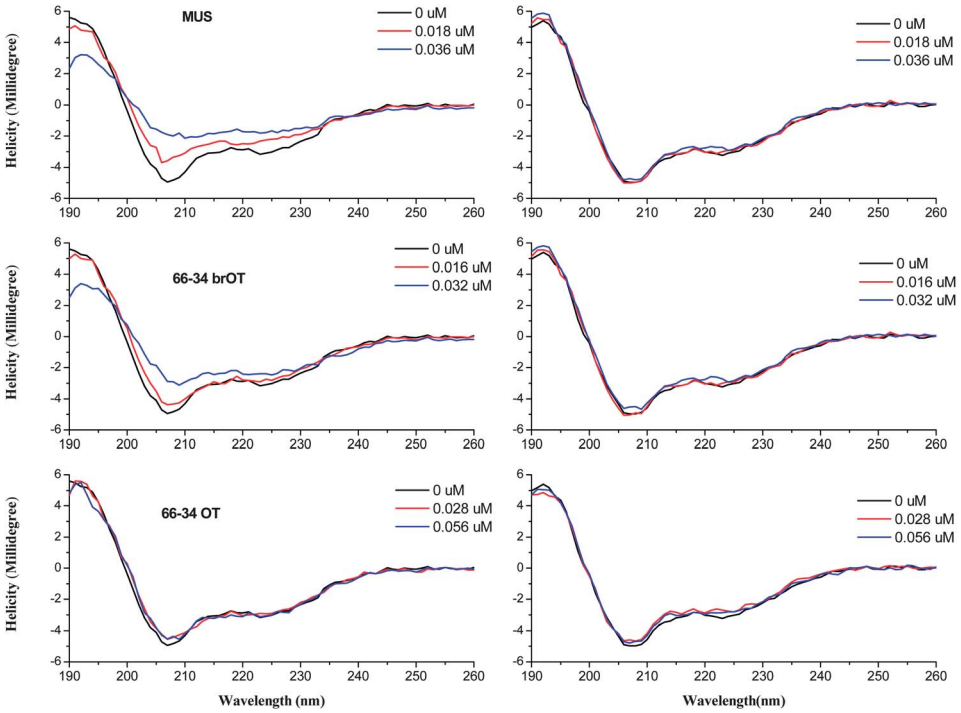

Fig. 3 CD spectra of ubiquitin at pH 4.0 (left) and 7.4 (right) in the presence of varying AuNP concentrations.

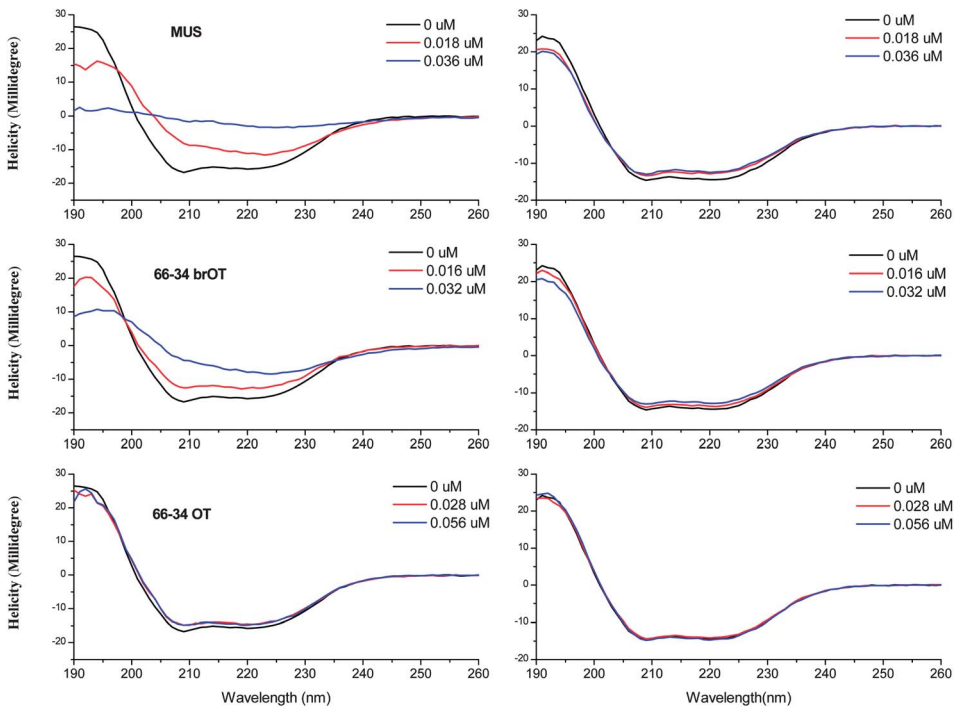

Fig. 4 CD spectra of fibrinogen at pH 4.0 (left) and 7.4 (right) in the presence of varying AuNP concentrations.

in solution, from these other thermodynamic quantities can be derived. These parameters reveal the mechanism of interaction in a quantitative manner, which makes ITC an excellent complement to other techniques. Therefore, it has been widely used to characterize protein–NP interaction.[2,30–32] Interaction of proteins with particles and surface is a complex process that not only involves the synergetic work of noncovalent forces including van der Waals force, hydrogen bonding, electrostatic and hydrophobic interactions, but also involves the desolvation of both NPs and proteins and solvation of newly formed

complexes.[31] Depending on the structure of the proteins and the properties of the interacting surface, the relative importance of each noncovalent force is altered, and they contribute differently to the heat profile measured by ITC. Noncovalent interactions are exothermic ($\Delta H < 0$), while the disruption of structurally well-defined solvent shells is endothermic ($\Delta H > 0$).

The heat profiles of the titration of the two proteins into the three types of AuNPs are presented in Fig. 5 and in the ESI (Fig. S2–S4†). The heat change profiles were satisfactorily fitted using isothermal functions to a model describing a single set of binding sites and best-fit parameters were calculated using nonlinear least-squares fitting (Tables 1 and 2). The thermodynamic quantities showed that the adsorption of ubiquitin onto all types of AuNPs featured a favorable enthalpy change ($\Delta H < 0$), which was offset partially by unfavorable entropy loss ($\Delta S < 0$), resulting in an overall negative free energy change ($\Delta G < 0$). Considering that the $-SO_3^-$ terminal group covered the entire MUS surface and 67% of the surface of the other two types of AuNPs, the adsorption of ubiquitin onto AuNPs seems to be primarily driven by electrostatic interaction.

Although the interactions of the proteins with all three types of AuNPs were consistently exothermic, differences existed between different types of proteins and AuNPs as shown in the thermodynamic parameters derived from the heat profiles (Tables 1 and 2). For ubiquitin adsorbed onto MUS and OT particles, although the associated constant, free energy change, and enthalpy change were not significantly different from each other, there were roughly 6 ubiquitins associated with MUS and only 3 ubiquitins attached per 66-34 OT particle. The thermodynamic parameters (ΔG, ΔH and $T\Delta S$) were all normalized per titrant (*i.e.*, the proteins). The similarity in these parameters suggests that the ubiquitins were adsorbed equivalently onto MUS and 66-34 OT. The similarity and difference between MUS and 66-34 OT in their interactions with ubiquitin are most likely originated from the difference in their surfaces. MUS particles were homogeneously coated with only 11-mercapto undecanesulfonate (MUS) ligands that end with $-SO_3^-$, ubiquitin "recognized" no difference on the surface of the particles and all the ubiquitins attached equivalently. In contrast, the 66-34 OT particles coated with a mixture of MUS and octanethiol (OT) were found to form stripe-like domains in the particles' ligand shell.[15] It is likely that ubiquitin selectively adsorbed close to the $-SO_3^-$ domains consequently finding fewer available sites as compared to that of MUS. For ubiquitin adsorbed onto 66-34 brOT particles, the enthalpy and entropy change is smaller than that of the other two systems, while there were more ubiquitins (~9) attached to each 66-34 brOT particle (Table 1). Compared to MUS particles with only one type of ligand and 66-34 OT particles with stripes at the nanoscale on the surface, 66-34 brOT particles have a mixture of MUS and 3,7-dimethyloctanethiol (brOT) that randomly distribute on its surface, forming molecular scale heterogeneity. Although ubiquitin also "recognized" no difference on the surface of 66-34 brOT (with a mixing of $-CH_3$ and $-SO_3^-$) since the contact area is possibly much larger than the molecular scale heterogeneity, it may use a different site to adsorb onto 66-34 brOT compared to its adsorption onto MUS and 66-34 OT particles, which with only $-SO_3^-$ available for adsorption. This is possibly responsible for the lower enthalpy and entropy in 66-34 brOT compared to the other two.

For fibrinogen adsorbed onto the three types of AuNPs, the association constant, enthalpy and entropy change are about an order of magnitude larger than that of ubiquitin, and about two AuNPs attached to one fibrinogen. This is consistent with the results from a recent study, which also reported a AuNP–fibrinogen molar ratio of 2 : 1 for 7 nm AuNPs.[33] Interestingly,

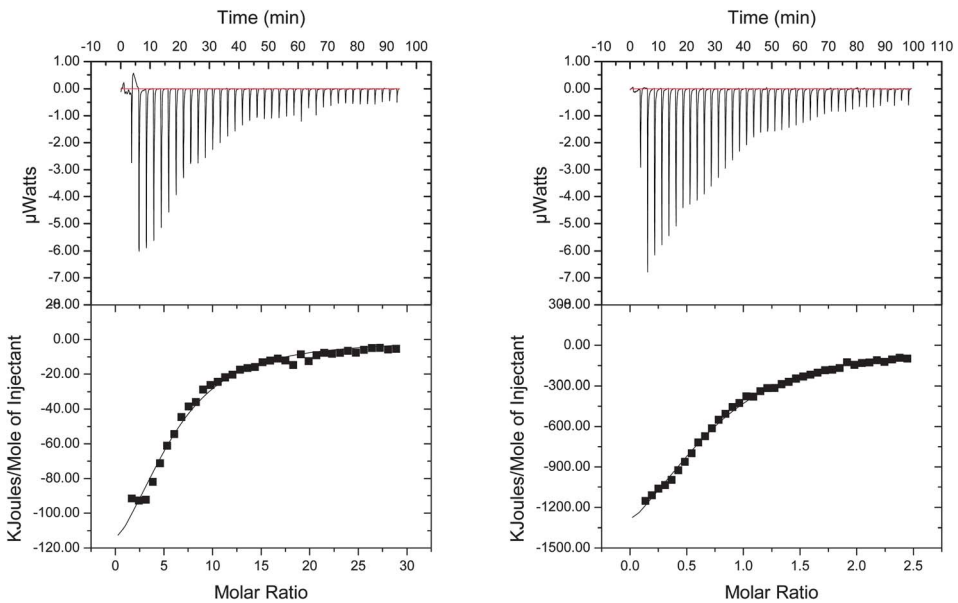

Fig. 5 ITC data from the titration of 1 mmol L^{-1} ubiquitin (left) and 80 µmol L^{-1} fibrinogen (right) into 7.03 µmol L^{-1} MUS AuNP. Heat flow *versus* time during injection of proteins at 25 °C and heat evolved per mole of added proteins (corrected for the heat of protein dilution) against the molar ratio (protein–AuNP) for each injection are shown at the top and bottom, respectively. The line is the model fitting (the data corresponding to the heat profile of dilution of protein are shown in the ESI Fig. S2†).

Table 1 Thermodynamic quantities of ubiquitin–AuNP interaction derived from ITC (error bar represents the variation between duplicate experiments)

NPs	K_s ($\times 10^5$ M^{-1})	$-\Delta G$ (kJ mol^{-1})	$-\Delta H$ (kJ mol^{-1})	$-T\Delta S$ (kJ mol^{-1})	n
MUS	0.57 ± 0.06	27.3 ± 0.3	149.5 ± 27.1	122.2 ± 27.4	6.18 ± 0.82
66-34 brOT	1.14 ± 0.35	28.8 ± 0.8	90.8 ± 5.4	62.1 ± 4.9	9.68 ± 1.37
66-34 OT	0.66 ± 0.09	27.5 ± 0.2	195.0 ± 5.7	167.0 ± 5.5	3.31 ± 0.57

Table 2 Thermodynamic quantities of fibrinogen–AuNP interaction derived from ITC (error bar represents the variation between duplicate experiments)

NPs	K_s ($\times 10^5$ M^{-1})	$-\Delta G$ (kJ mol^{-1})	$-\Delta H$ (kJ mol^{-1})	$-T\Delta S$ (kJ mol^{-1})	n
MUS	6.46 ± 3.29	31.64 ± 0.89	1786.0 ± 182.4	1753.7 ± 183.3	0.78 ± 0.10
66-34 brOT	8.05 ± 0.73	57.0 ± 27.7	1702.0 ± 364.8	1645.0 ± 337.1	0.83 ± 0.11
66-34 OT	8.49 ± 0.89	33.7 ± 0.5	1704.0 ± 31.1	1670.3 ± 31.6	0.54 ± 0.01

there is no significant difference between the adsorption onto the three types of AuNPs (Table 2). It is probably due to the relatively large size of fibrinogen (340 kD) compared to ubiquitin (8.5 kD). For each fibrinogen molecule, there were more electrostatic interactions involved compared to each ubiquitin molecule, as it wrapped two AuNPs, so the enthalpy and entropy change is much larger than that of ubiquitin. Since the contact area between fibrinogen and the AuNPs is much larger than the surface features of the AuNPs, fibrinogen "recognized" no difference on the surfaces of both 66-34 brOT and 66-34 OT. As a result, they interacted in the same way as that between fibrinogen and the homogeneously charged MUS.

3.5 Scale-dependency of surface heterogeneity

Results from the present study demonstrated that the structural and compositional heterogeneity on the surface of both proteins and NPs have great influence on their interaction. For proteins, their stability in electrolytes can be largely attributed to the heterogeneity, as the surface heterogeneity may provide them forces other than van der Waals force and electrostatic interaction.[34,35]

At neutral pH, although there are positively charged residues exposed and available for interacting with negatively charged surface, the negatively charged residues can help to maintain the repulsion between the protein and the negatively charged particle. As pH decreased and most carboxyl groups became protonated (*e.g.*, side chain of aspartic acid and glutamic acid), the surface charge heterogeneity was reduced, resulting in a tighter interaction between the proteins and AuNPs and the disruption of protein structure.

The protein adsorption results from the present study demonstrated the scale dependency of protein adsorption, and the scale is determined by both protein and the interaction surface. The size and shape of protein, and the size of surface features determine the potential contact area between them. The size of ubiquitin is around 1.5 nm and the contact area is possibly at the sub-nanoscale, which is comparable to the surface features on the particle surface. The stripe-like domain of the 66-34 OT particle is around 0.5 nm and the surface feature of 66-34 brOT is at the molecular scale. The protein "recognizes" the difference between these surfaces and shows different adsorption behaviors, as the ITC results suggested. However, when the size of the protein or the contact area is much larger than the surface features, like fibrinogen in this case may wrap around the particles, the protein "recognizes" no difference between these surfaces, and the adsorption behavior will be very likely the same.

A similar scale-dependent protein adsorption phenomenon has recently been explored theoretically through molecular dynamic simulation.[36,37] For particles similar to those used in this study, the amphiphilic side chains of lysine and arginine were found to respectively direct the interaction of cytochrome C and lysozyme with the particles, and the interaction modes (residues in contact with the particle surface and the geometry of the adsorbed protein) depend on the size of the surface structure.

4 Conclusion

The interactions between two common serum proteins (ubiquitin and fibrinogen) and three types of AuNPs were investigated. Both ubiquitin and fibrinogen can adsorb onto the three types of AuNPs at pH above and below the IEPs of the proteins, and the interaction may be predominantly electrostatic through some positive patches of the proteins (*e.g.*, sites with side chains of lysine or arginine). However, surface charge heterogeneity strongly affected the interaction and the structure of the proteins. The protonation or deprotonation as a result of pH change modulates the surface charge of proteins, which determines the structural stability of the adsorbed proteins.

The adsorption of ubiquitin and fibrinogen on the AuNPs was found to be influenced by the surface chemistry and structure of the AuNPs, especially the scale of surface heterogeneity. Ubiquitin, a small protein that has comparable size to the surface features of the AuNPs, adsorbed differently (in terms of binding stoichiometry and thermodynamics) onto (1) AuNPs with charged and nonpolar terminals organized into the nanoscale structure (66-34 OT), (2) AuNPs with randomly distributed

terminals (66-34 brOT), and (3) AuNPs with homogeneously charged terminals (MUS). Fibrinogen, which is much larger than the surface features of the AuNPs, possessed similar adsorption behaviors onto the three types of AuNPs. Results from this study demonstrated the importance of the surface structure in addition to the surface chemical composition in determining NP–protein interactions.

Acknowledgements

The authors would like to thank Dr Craig J. Moehnke for his assistance in using various spectroscopy instruments and also thank Dr Stella Marinakos for the TEM characterization of the three types of AuNPs. RPC and FS would like to acknowledge the Swiss National Foundation NRP 64 program for supporting this work.

References

1 A. E. Nel, L. Madler, D. Velegol, T. Xia, E. M. V. Hoek, P. Somasundaran, F. Klaessig, V. Castranova and M. Thompson, *Nat. Mater.*, 2009, **8**, 543–557.
2 S. P. Singh, S. Chakraborty, P. Joshi, V. Shanker, Z. A. Ansari and P. Chakrabarti, *Langmuir*, 2011, **27**, 7722–7731.
3 F. Meder, T. Daberkow, L. Treccani, M. Wilhelm, M. Schowalter, A. Rosenauer, L. Madler and K. Rezwan, *Acta Biomater.*, 2012, **8**, 1221–1229.
4 S. H. D. Lacerda, J. J. Park, C. Meuse, D. Pristinski, M. L. Becker, A. Karim and J. F. Douglas, *ACS Nano*, 2010, **4**, 365–379.
5 M. Lundqvist, J. Stigler, G. Elia, I. Lynch, T. Cedervall and K. A. Dawson, *Proc. Natl. Acad. Sci. U. S. A.*, 2008, **105**, 14265–14270.
6 S. Pereira, A. Zille, E. Micheletti, P. Moradas-Ferreira, R. De Philippis and P. Tamagnini, *FEMS Microbiol. Rev.*, 2009, **33**, 917–941.
7 E. Tombacz and M. Szekeres, *Appl. Clay Sci.*, 2006, **34**, 105–124.
8 M. Zembala, *Adv. Colloid Interface Sci.*, 2004, **112**, 59–92.
9 J. Y. Walz, *Adv. Colloid Interface Sci.*, 1998, **74**, 119–168.
10 J. Drelich, J. L. Wilbur, J. D. Miller and G. M. Whitesides, *Langmuir*, 1996, **12**, 1913–1922.
11 R. Duffadar, S. Kalasin, J. M. Davis and M. M. Santore, *J. Colloid Interface Sci.*, 2009, **337**, 396–407.
12 G. Hodgkinson and V. Hlady, *J. Adhes. Sci. Technol.*, 2005, **19**, 235–255.
13 T. C. Ta and M. T. McDermott, *Anal. Chem.*, 2000, **72**, 2627–2634.
14 A. M. Jackson, Y. Hu, P. J. Silva and F. Stellacci, *J. Am. Chem. Soc.*, 2006, **128**, 11135–11149.
15 O. Uzun, Y. Hu, A. Verma, S. Chen, A. Centrone and F. Stellacci, *Chem. Commun.*, 2008, 196–198.
16 A. Verma, O. Uzun, Y. H. Hu, Y. Hu, H. S. Han, N. Watson, S. L. Chen, D. J. Irvine and F. Stellacci, *Nat. Mater.*, 2008, **7**, 588–595.
17 A. Centrone, E. Penzo, M. Sharma, J. W. Myerson, A. M. Jackson, N. Marzari and F. Stellacci, *Proc. Natl. Acad. Sci. U. S. A.*, 2008, **105**, 9886–9891.
18 J. J. Kuna, K. Voitchovsky, C. Singh, H. Jiang, S. Mwenifumbo, P. K. Ghorai, M. M. Stevens, S. C. Glotzer and F. Stellacci, *Nat. Mater.*, 2009, **8**, 837–842.
19 X. Liu, M. Yu, H. Kim, M. Mameli and F. Stellacci, *Nat. Commun.*, 2012, **3**, 1182.
20 S. Vijaykumar, C. E. Bugg and W. J. Cook, *J. Mol. Biol.*, 1987, **194**, 531–544.
21 V. N. Uversky, *Biochemistry*, 1993, **32**, 13288–13298.
22 C. Fuss, J. C. Palmaz and E. A. Sprague, *J. Vasc. Intervent. Radiol.*, 2001, **12**, 677–682.
23 M. Wasilewska, Z. Adamczyk and B. Jachimska, *Langmuir*, 2009, **25**, 3698–3704.
24 F. Rossi, L. Calzolai, F. Franchini and D. Gilliland, *Nano Lett.*, 2010, **10**, 3101–3105.
25 H. Jans, X. Liu, L. Austin, G. Maes and Q. Huo, *Anal. Chem.*, 2009, **81**, 9425–9432.
26 V. A. Hackley, D. H. Tsai, F. W. DelRio, A. M. Keene, K. M. Tyner, R. I. MacCuspie, T. J. Cho and M. R. Zachariah, *Langmuir*, 2011, **27**, 2464–2477.
27 D. C. Carter and J. X. Ho, *Adv. Protein Chem.*, 1994, **37**, 153–203.
28 R. Cukalevski, M. Lundqvist, C. Oslakovic, B. Dahlback, S. Linse and T. Cedervall, *Langmuir*, 2011, **27**, 14360–14369.
29 S. J. Dong, L. Shang, Y. Z. Wang and J. G. Jiang, *Langmuir*, 2007, **23**, 2714–2721.
30 S. Lindman, I. Lynch, E. Thulin, H. Nilsson, K. A. Dawson and S. Linse, *Nano Lett.*, 2007, **7**, 914–920.
31 M. De, C.-C. You, S. Srivastava and V. M. Rotello, *J. Am. Chem. Soc.*, 2007, **129**, 10747–10753.
32 T. Cedervall, I. Lynch, S. Lindman, T. Berggård, E. Thulin, H. Nilsson, K. A. Dawson and S. Linse, *Proc. Natl. Acad. Sci. U. S. A.*, 2007, **104**, 2050–2055.
33 Z. J. Deng, M. T. Liang, I. Toth, M. J. Monteiro and R. F. Minchin, *ACS Nano*, 2012, **6**, 8962–8969.
34 A. J. Rowe, *Biophys. Chem.*, 2001, **93**, 93–101.
35 M. Bostrom, D. R. M. Williams and B. W. Ninham, *Phys. Rev. Lett.*, 2001, **8716**, 168103.
36 A. Hung, S. Mwenifumbo, M. Mager, J. J. Kuna, F. Stellacci, I. Yarovsky and M. M. Stevens, *J. Am. Chem. Soc.*, 2011, **133**, 1438–1450.
37 A. Hung, M. Mager, M. Hembury, F. Stellacci, M. M. Stevens and I. Yarovsky, *Chem. Sci.*, 2013, **4**, 928–937.